Multi-Detector Analyses for CCSN Neutrino Detection.

Meriem Bendahman[1,4][0000−0002−2730−3445], Isabel Goos[1][0009−0008−1479−539X], Joao Coelho[1][0000−0001−5615−3899], Matteo Bugli[2,3][0000−0002−7834−0422], Alexis Coleiro[1][0000−0003−0860−440X], Sonia El Hedri[1][0000−0002−1728−8843], Thierry Foglizzo[3][0000−0001−5869−8518], Davide Franco[1][0000−0001−5604−2531], Jérôme Guilet[3][0000−0002−7518−8752], Antoine Kouchner[1][0000−0001−7068−2113], Raphaël Raynaud[6][0000−0001−6815−7109], and Yahya Tayalati[4,5][0000−0001−8760−7259]

[1] Université Paris Cité, CNRS, Astroparticule et Cosmologie, F-75013 Paris, France
[2] Dipartimento di Fisica, Università di Torino, I-10125 Torino, Italy
[3] Université Paris-Saclay, Université Paris Cité, CEA, CNRS, AIM, 91191, Gif-sur-Yvette, France
[4] Faculty of Sciences, Mohammed V University in Rabat, Avenue des Nations Unies, Rabat, Morocco
[5] Institute of Applied Physics, Mohammed VI Polytechnic University, Ben Guerir, Morocco
[6] Université Paris Cité, Université Paris-Saclay, CEA, CNRS, AIM, F-91191 Gif-sur-Yvette, France
mbendahman@km3net.de

Abstract. Core-collapse supernovae (CCSNe) represent significant astronomical occurrences that offer essential insights into galaxy dynamics. The temporal pattern of neutrinos during these events serves as a distinctive and valuable information source, shedding light on collapsing star mechanisms and particle behaviors in densely packed environments. Despite the rarity of nearby supernovae, only one observation of supernova neutrinos has been recorded to date. To optimize our understanding during the next galactic CCSN, it is crucial to amalgamate real-time observations from multiple neutrino experiments and promptly convey the results to optical telescopes. However, pinpointing the CCSN poses a substantial challenge, requiring the separation of localization information from signatures associated with supernova progenitor properties or neutrino physics. Existing CCSN distance measurement algorithms assume accurate predictions of neutrino properties by the Standard Model. This contribution introduces an approach to rapidly and effectively extract and distinguish information about CCSN and neutrino physics. We demonstrate the robustness of this approach against potential biases in CCSN measurements due to new physics effects, leveraging the diverse capabilities of next-generation neutrino detectors.

Keywords: Core-Collapse Supernova · Mass ordering · Neutrino two-body decays.

1 Introduction

Core-collapse supernovae (CCSNe) offer important insights into the dynamics of galaxies. Detecting the neutrino burst from a potential CCSN in the Milky Way before the visible explosion occurs is theoretically possible. Given the infrequency of galactic supernovae, it is crucial to promptly extract reliable CCSN localization information from neutrino data and transmit it efficiently to telescopes. Understanding the CCSN distance holds particular importance, as it could help ascertain whether the supernova took place in the dust-obscured regions behind the galactic center, influencing observation strategies [1]. However, untangling the impact of this distance from the effects of progenitor and neutrino properties on observations presents substantial challenges. Existing strategies for CCSN distance measurement aim to mitigate progenitor dependence but rely on the assumption of standard neutrino flavor conversion mechanisms [2, 3]. Approaches to constrain neutrino properties often hinge on energy measurements [4], a variable that may not be universally available across all experiments. Over the next two decades, the field of neutrino detectors sensitive to CCSNe will undergo a significant transformation, introducing new detectors sensitive to various combinations of neutrino flavors alongside traditional water Cherenkov detectors. This flavor complementarity could potentially break degeneracies between neutrino and CCSN properties even when the event energies are not known, thus improving the robustness of the CCSN distance measurements made by the Supernova Early Warning System (SNEWS) [5]. In this contribution, we introduce an algorithm designed to simultaneously constrain CCSN position, progenitor characteristics, and neutrino properties, utilizing only neutrino counting rates measured at large-scale next-generation experiments. We assess the algorithm's capability to locate CCSNe and characterize neutrinos with minimal information, while also evaluating its robustness in the presence of non-standard interactions such as neutrino two-body decays.

2 Methodology

In examining the effects of CCSN and neutrino properties on observations, we assess the anticipated neutrino rates across various current and upcoming experiments, employing a diverse range of supernova models and different flavor conversion mechanisms. This section outlines the methodology involved in this assessment and details the observables selected for characterizing CCSN.

CCSN Models: In this analysis, we explore a collection of 149 progenitor models formulated and introduced in [6]. These models, established through one-dimensional simulations, encompass a broad spectrum of progenitor parameters such as masses, compactness, and metallicity, which are anticipated in CCSNe with an iron core. The purpose behind their creation was to identify observables with a weak dependence on the CCSN model, making them particularly well-suited for our study. The probability distribution for these models is defined using the Salpeter Initial Mass Function: $w(M) \propto M^{-2.35}$, M is the progenitor

mass.

Neutrino Experiments: Future large-scale detectors will exhibit sensitivity to three neutrino flavor combinations. Water Cherenkov (WC) detectors will be responsive to electron antineutrinos, kiloton-scale liquid argon detectors to electron neutrinos, and detectors for Coherent Neutrino-Nucleus scattering (CEνNS) will be sensitive to the sum of all neutrino flavors. In the case of WC detectors, our considerations include Hyper-Kamiokande (HK), IceCube, and KM3NeT. Large liquid argon experiments focus on DUNE's far detector, currently the most extensive project in this category. Additionally, for CEνNS detection experiments, we examine DarkSide-20k and a comparable but seven times larger project named ARGO.

Neutrino Flavor Conversion Models: This analysis specifically delves into the initial 150 milliseconds of a CCSN, where adiabatic MSW flavor transitions predominantly govern flavor-conversion mechanisms within the star. The MSW effect strongly depends on the mass ordering. Furthermore, we explore scenarios involving two-body decays of neutrinos. This BSM scenario represents one example of new physics phenomena which can mimic SM scenarios and introducing biases in distance and mass ordering estimates [7]. As an example, we consider the Dirac ϕ_0 scenario from [7], where the heaviest neutrino species decays into the lightest, introducing two parameters: the ratio $\bar{r}$ of the CCSN distance over the decay length and the branching ratio ζ to active neutrinos.

Analysis Pipeline: Neutrino rates at various detectors are evaluated using the SNEWPY software [8]. SNEWPY has been modified to incorporate the described neutrino decay model, along with detection efficiency curves for DarkSide-20k and ARGO [9]. For IceCube and KM3NeT, Poissonian backgrounds are added, with rates of 1.5 MHz and 4.5 MHz, respectively.

Building Block Observables: This analysis relies on observables with low or easily parameterizable dependencies on the CCSN model. Many of these observables, known as "standard candles" for CCSN distance measurements at single detectors, have been proposed in previous literature [2, 3]. While earlier time windows display weaker CCSN model dependence, the reduced statistical uncertainties for larger windows might lead to more precise measurements. Additionally, we examine ratios between the rates described above and those measured during the early accretion phase, specifically 100 to 150 milliseconds after the beginning of the CCSN. This choice, aims to mitigate the residual model-dependence of early neutrino rates for CCSN distance measurements. The associated observables, referred to as f_Δ and illustrated in figure 1, exhibit quasi-linear dependence on early neutrino rates.

$$f_\Delta(\Delta t) = \frac{N(100 - 150 \text{ ms})}{N(\Delta t)} \approx \alpha N(\Delta t) + \beta \tag{1}$$

In the study by [2], a value of Δt was set at 50 milliseconds.

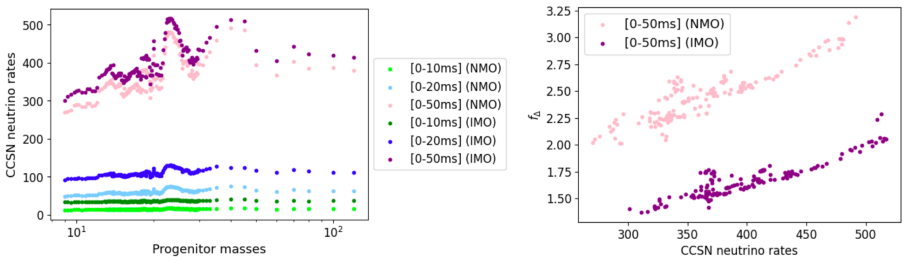

Fig. 1. Left: CCSN neutrino rates in Hyper-Kamiokande for a CCSN at 10 kpc as a function of progenitor masses, for the first 10 ms (green), 20 ms (blue), and 50 ms (purple) postbounce. Right: f_Δ as a function of the number of CCSN neutrino events in the first 50 ms. NMO and the IMO, are presented with light and dark colors respectively.

3 Likelihood analysis

Considering a set of neutrino detectors, we establish the following likelihood function:

$$\log \mathcal{L}(\{\mathcal{O}_{\rm obs}\}|d, M, \bar{r}, \zeta, \mathrm{MO}) = \sum_i \log P[N_i(10ms)] + \log P[N_i(10-20ms)] + \log P[N_i(20-50ms)] + \log P[N_i(100-150ms)] \quad (2)$$

The index i represents the individual neutrino detectors, M and d represent the progenitor mass, and the supernova distance, respectively. The parameters $(\bar{r}, \zeta)$ correspond to the neutrino decay parameters. P denotes the Poisson probability distribution for observing a specific count of events:

$$P(N_i) = \frac{\lambda_i^{N_i} e^{-\lambda_i}}{N_i!}, \quad (3)$$

$\lambda_i(d, M, \bar{r}, \zeta, \mathrm{MO})$ is the expected value of N_i considering CCSN and neutrino properties, $\{\mathcal{O}_{\rm obs}\}$ denotes the collection of measurements conducted for various detectors. When constraining a specific parameter, such as θ or the CCSN distance, the remaining parameters are regarded as nuisance parameters Ξ. In this context, we establish a profile likelihood:

$$\mathcal{L}_{\rm prof}(\{\mathcal{O}_i\}|\theta) = \max_\Xi \mathcal{L}(\{\mathcal{O}_i\}|\theta, \Xi) \quad (4)$$

which can be used for either parameter fitting or hypothesis testing. To optimize the likelihood over $(\bar{r}, \zeta)$, a regular grid is considered, where: $\Delta\bar{r} = 0.05$ and $\Delta\zeta = 0.1$.

4 Mass ordering determination

We employ the likelihood specified in equation 2 to deduce the neutrino Mass Ordering (MO) without knowledge of the CCSN distance. Initially assuming

that neutrino properties follow to the Standard Model (SM), we maximize the likelihood over distances and supernova models for each mass ordering (MO) hypothesis given a particular measurement. Subsequently, we compute the p-value for a IMO or NMO measurement, using the ratio of IMO and NMO likelihoods as test statistic defined as:

$$t(\{\mathcal{O}_{\rm obs}\}) = \frac{\max_{d,M,\bar{r},\zeta}\left[\mathcal{L}(\{\mathcal{O}_{\rm obs}\}|d,M,\bar{r},\zeta,{\rm NMO})\right]}{\max_{d,M,\bar{r},\zeta}\left[\mathcal{L}(\{\mathcal{O}_{\rm obs}\}|d,M,\bar{r},\zeta,{\rm IMO})\right]} \tag{5}$$

The likelihoods are optimised over both CCSN distance and the CCSN models. In the scenario of the Standard Model, the parameters are set to $\bar{r} = 0$ and $\zeta = 1$. However, if the potential for neutrino decays is taken into consideration, the likelihoods are optimised over the $\bar{r}$ and ζ parameters. To assess the probability distribution of t under a specific mass ordering hypothesis, we generate potential observations by sampling from a prior probability distribution described in [10]. Figure 2 illustrates the 3σ distance horizon for rejecting the IMO based on a typical NMO measurement, considering both single and pairs of experiments. Combining Hyper-Kamiokande and IceCube extends the distance horizon from 20 kpc, when considering Hyper-Kamiokande alone, to 23 kpc. Notably, the most significant enhancement occurs when combining Hyper-Kamiokande with DUNE, resulting in a 27 kpc horizon that encompasses the entire galaxy. Likewise, for the IMO, the 3 distance horizon extends from 11 kpc to 18 kpc when combining DUNE with ARGO and from 14kpc to 19 kpc when pairing DUNE with IceCube. We then assess the ability of neutrino experiments to differentiate between the NMO and the IMO scenarios, considering the presence of neutrino decays. The right panel of Figure 2 displays the corresponding distance horizons for rejecting the Standard Model in the IMO. In this analysis, we simulated an observation for which $\bar{r} = 5, \zeta = 1$, but we vary $\bar{r}$ and ζ when we optimize the likelihood. For IMO rejection, the largest distance horizons are achieved by combining DUNE with HK (22 kpc) and by combining HK with ARGO (21 kpc).

5 Measuring supernova distances

To investigate the effect of neutrino decays on CCSN distance measurements, we examine a representative measurement for an 11 $M_\odot$ progenitor, considering a specific neutrino decay scenario ($\bar{r} = 5$ and $\zeta = 1$). In Figure 3, the measured CCSN distance and the corresponding 90% confidence interval are depicted as functions of the true distance for the IMO scenario with ($\bar{r} = 5, \zeta = 1$). In Figure 3, the measured CCSN distance and the corresponding 90% confidence interval are depicted as functions of the true distance for the IMO scenario with ($\bar{r} = 5, \zeta = 1$) mentioned earlier. This analysis is conducted for the DUNE and HK detectors individually, as well as for their combined results. In this figure, the distance estimated using the SM-only likelihood is compared to the distance obtained by allowing $\bar{r}$ and ζ to vary. For both DUNE and HK, a noticeable bias in the distance measurement is evident under the SM assumption. This bias

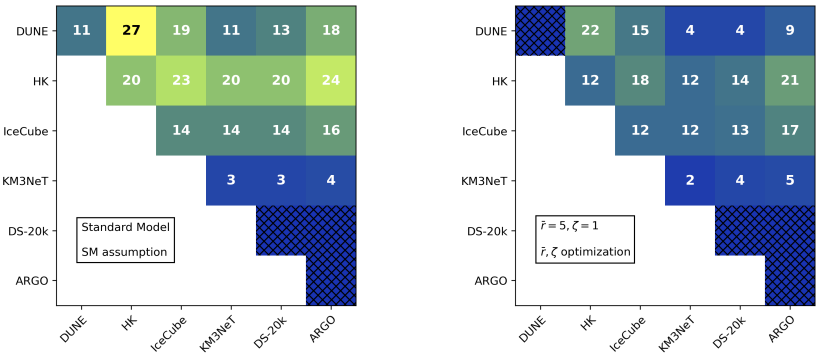

Fig. 2. 3σ distance horizon (measured in kpc) indicating the rejection for the IMO when the NMO is the true mass ordering. The individual detectors are shown in the diagonal, off-diagonal elements display pairs of detectors. The cross-hatched regions identify experiments or pairs of experiments lacking sensitivity to the mass ordering, such as DUNE in the presence of neutrino decays, and CEνNS experiments like ARGO and DarkSide-20k. Left: Standard Model scenario utilizing a SM likelihood. Right: Beyond Standard Model scenario with $\bar{r} = 5, \zeta = 1$, with $\bar{r}$ and ζ treated as degrees of freedom in the likelihood.

can be, to some extent, rectified by incorporating $\bar{r}$ and ζ parameters in the CCSN distance fitting process. . In that case, when combining DUNE and HK, the 90% C.L. uncertainties become comparable to the ones obtained under the SM assumption.

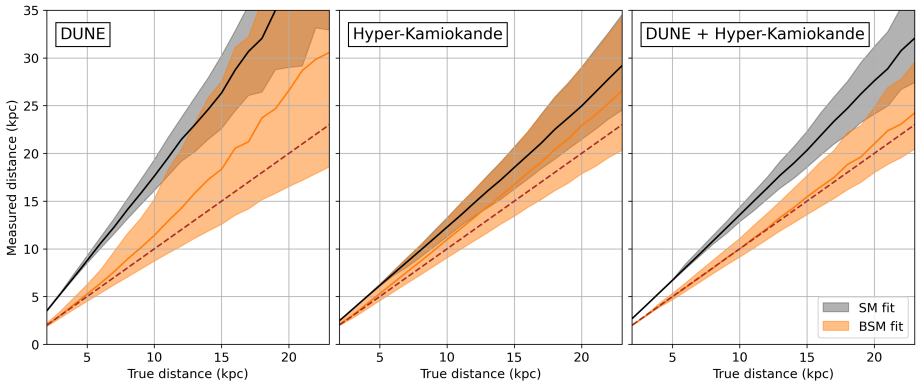

Fig. 3. Median values and 90% confidence intervals on the measured CCSN distance are presented as functions of the true distance, for a $11M_{\odot}$ progenitor, assuming the IMO and a neutrino decay model of $\bar{r} = 5, \zeta = 1$. DUNE, HK and their combination are presented. The grey band is for the SM hypothesis, while the orange band is a fit where $\bar{r}$ and ζ are optimized alongside the other parameters.

6 Conclusion

In this contribution, we demonstrated that with a method using a minimal set of observables, and exploiting the capabilities of the next generation of neutrino experiments, the CCSN alert systems impose constraints on CCSN properties even when the energies of the detected events are unknown. Taking neutrino decays an example, we showed how new physics in the neutrino sector can introduce notable biases into CCSN distance estimates. We also have demonstrated that when new physics impacts neutrino fluxes in a flavor-dependent manner, it becomes possible to correct distance estimates while maintaining control over uncertainties. This correction can be achieved through the combination of flavor-complementary neutrino detectors.

Acknowledgements This work is supported by LabEx UnivEarthS (ANR-10-LABX-0023 and ANR-18-IDEX-0001) and Paris Region (DIM ORIGINES). We thank Gwenhaël de Wasseige, Maria Cristina Volpe and Joachim Kopp for interesting and helpful discussions. This project has received funding from the European Union's Horizon Europe research and innovation programme under the Marie Skłodowska-Curie grant agreement No 101064953 (GR-PLUTO). Joao Coelho, Alexis Coleiro, Sonia El Hedri, Davide Franco, Isabel Goos and Antoine Kouchner are supported by Centre National de la Recherche Scientifique (CNRS). The Moroccan Ministry of Higher Education, Scientific Research and Innovation is acknowledged.

References

1. K. Nakamura *et al*, Mon. Not. Roy. Astron. Soc. **461** (2016) no.3, 3296-3313.
2. M. Segerlund *et al.*, arXiv:2101.10624v1 [astro-ph.HE].
3. M. Kachelriess *et al.*, Phys. Rev. D 71 (2005) 063003.
4. X.-R. Huang *et al.*, arXiv:2305.00392 [hep-ph].
5. SNEWS Collaboration, New J. Phys. 23 (2021).
6. T. Sukhbold, *et al.*, Astrophys. J. 821, 38 (2016).
7. A. de Gouvea *et al.*, Phys. Rev. D 101 (2020) 4, 043013.
8. A. Baxter *et al.*, J. Open Source Softw. **6** (2021) no. 67, 3772.
9. DarkSide Collaboration, JCAP 03 (2021) 043.
10. M.Bendahman *et al.*, JCAP 02 (2024) 008.